Generic Algorithm for Peg-In-Hole Assembly Tasks for Pin Alignments with Impedance Controlled Robots

Michael Jokesch, Jozef Suchý, Alexander Winkler, André Fross and Ulrike Thomas

Abstract In this paper, a generic algorithm for peg-in-hole assembly tasks is suggested. It is applied in the project GINKO were the aim is to connect electric vehicles with charging stations automatically. This paper explains an algorithm applicable for peg-in-hole tasks by means of Cartesian impedance controlled robots. The plugging task is a specialized peg-in-hole task for which 7 pins have to be aligned simultaneously and the peg and the hole have asymmetric shapes. In addition significant forces are required for complete insertion. The initial position is inaccurately estimated by a vision system. Hence, there are translational and rotational uncertainties between the plug, carried by the robot and the socket, situated on the E-car. To compensate these errors three different steps of Cartesian impedance control are performed. To verify our approach we evaluated the algorithm from many different start positions.

Keywords Peg-In-Hole · Impedance control · Electric vehicles · Charging

1 Introduction

Many assembly tasks exist which are similar to peg-in-hole tasks. A specialized peg-in-hole tasks occurs when the robot takes a plug to connect it automatically to an E-car at a recharging station. In our project which is part of the GINKO project [3] we intent to build a force-fit and form-fit connection according to the norm DIN EN 62196-2. It is a big difference to recharging conventional fuels [1] [2] where the fuel hose diameter is much smaller than the tank opening. Considering this, we have high requirements on the accuracy of the positioning in our task (Fig. 1). The task can be

M. Jokesch(✉) · J. Suchý · A. Winkler · A. Fross · U. Thomas
Technische Universität Chemnitz, Reichenhainer Straße 70, 09126 Chemnitz, Germany
e-mail: {michael.jokesch,jozef.suchy,ulrike.thomas}@etit.tu-chemnitz.de,
winkler3@hs-mittweida.de, fross@coremountains.de
http://www.tu-chemnitz.de

This paper is supported by the Federal Ministry of Education and Research (Germany), under the funding code 03IPT505A. Responsibility for content lies with the authors.

L.P. Reis et al. (eds.), *Robot 2015: Second Iberian Robotics Conference*,
Advances in Intelligent Systems and Computing 418,
DOI: 10.1007/978-3-319-27149-1_9

classified as a complex peg-in-hole problem. The peg-in-hole task is well known from [5] [6] [7], representative for many more papers. Unfortunately, most of these solutions assume a cylindrical peg and a slightly enlarged cylindrical hole. Whitney [4] published an interesting approach with the idea of passive compliance that is also used in this work. In general, the insertion process is mostly divided into two phases. The search phase and the insertion phase.

During the search phase, the hole is detected and the peg center is moved toward the center of hole. The accuracy of this phase usually has to be within the clearance which is defined as the difference between the peg diameter and the hole diameter [5]. Approaches suggested to align the peg with the hole are using vision systems, force/torque information with blind-search-algorithms [6] or neural networks. An approach that uses a neural network was published by Newman [7]. The neural network takes a pre-recorded map of positions vs. torques as a basis.

Approaches with force/torque feedback, e.g. force/torque maps with particle filters [8], are very interesting when the vision system reaches its limits which could be caused by the illumination of the environment, the camera resolution, the field of view and/or the accuracy of hole detection. One disadvantage of the blind-search strategies can be the time duration. Depending on the size of the workspace and the uncertainties of prior positioning blind searching can be very time consuming. For smarter and more effective search, Newman et al. developed the strategy of position vs. torque map [7]. When the peg comes into contact with the surface the torques are measured and compared with the map. With this information it is calculated which direction has the highest probability for finding the hole. The big problem of this approach is its inflexibility. Already a small change in the workspace requires a complete recalibration of the map. Additionally, it is assumed that the peg has always the same orientation to the surface. In order to understand the peg-in-hole problems better and find new approaches the human behavior was analyzed several times, e.g. in [9], [10]. Although the peg-in-hole is an old problem in robotics [11] it is still an actual problem. This is why many groups still perform research into it [12], [13], [14].

The approaches presented above are not quite useful in solving our problem because the workspace changes steadily (different cars) and a simple blind-search is too time-consuming. Furthermore, we deal with valuable objects – cars, i.e. it has to be worked with high caution. Another important issue is the special shape of the charging plug (Fig. 1).

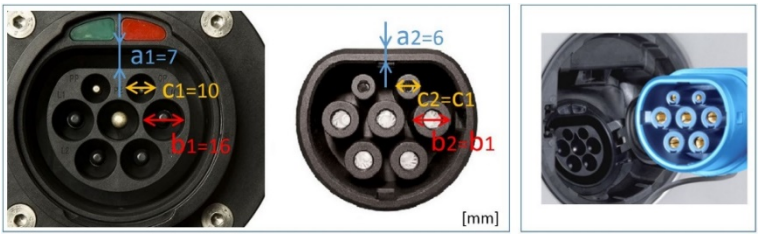

Fig. 1 Right image: EU standardized charging plug (blue) and plug socket (black) with 7 pins and a flattened side. The socket is situated at the car and the plug is moved by the robot. Left image: frontal view of the socket and the plug. b1/2 and c1/2 fit exactly (no clearance). Between a1 and a2 clearance is 1 mm which makes threading easier.

It has 7 different sized pins and a flattened side for protection against polarity reversal. During our research, we did not find work concerning the peg-in-hole task with such a high number of different pegs. The algorithm needs to compensate for translational and rotational displacements between the connector and the socket; otherwise the connection will not be possible. In [15] they use a kind of impedance control for peg-in-hole assembly of complex shaped workpieces. The impedance control method is used in our work in combination with a kind of blind-search algorithm. This gives rise to search strategy, which can be transferred to many other peg-in-hole problems with very small effort.

In the next section, the problem is discussed in more detail and the experimental set-up is presented. In Section 3 the proposed force/torque based control algorithm is explained and in Section 4 it is tested and evaluated. At the end the results are summarized and the conclusions are drawn.

2 Problem Formulation and Test Set-Up

The initial situation of this work is the prior coarse positioning by means of a vision system. The goal is to align plug's pose with socket pose and thus enable the robot to insert the charging plug into the plug socket. Differences between the poses are possible in every degree of freedom (DOF), see Fig. 2. These misalignments appear together, that means it is important that compensation works for every DOF simultaneously. There is no clearance between the pins and the holes. Only the external shape has a clearance value of 1 mm (shown in Fig. 1). After the alignment a force of 160 to 200 Newton in insertion direction is necessary for full connection. It results in a force closure connection. In summary, following steps need to be implemented:

- Apply vision for rough positioning (not presented in this paper)
- Using search strategies (align plug with socket)
- Establishing contact and insertion (generate required force in insertion direction)

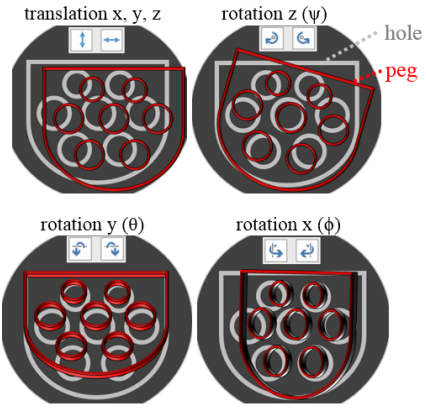

Fig. 2 Possible positioning errors due to the vision system

To analyze the algorithms we have built a test station in laboratory and also can work at a real electric car (Fig. 3). The position of the socket can easily be changed to simulate different initial situations. The Robot used for experiments is KUKA LWR iiwa 7 R800 with seven joints. Every joint is equipped with a torque sensor. Thus, it is possible to implement compliance control [16], which enables the proposed algorithm. The impedance control supports the insertion process and simultaneously protects the environment, e.g. car or human, from being damaged.

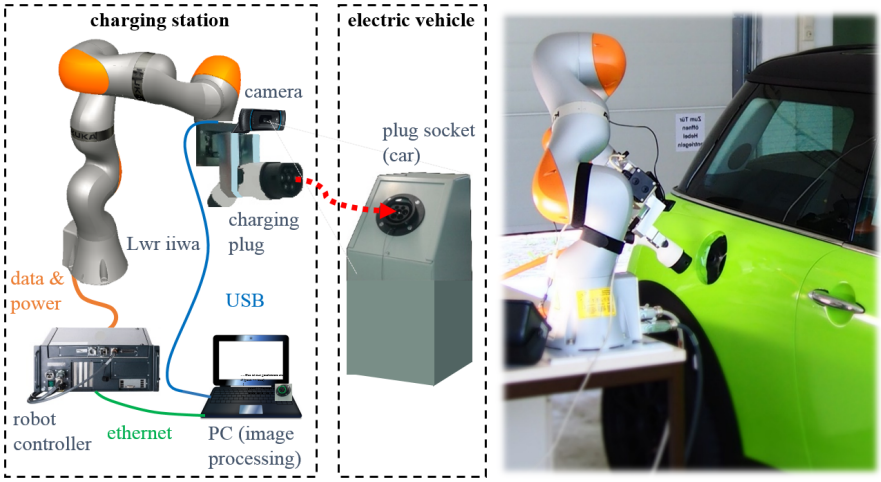

Fig. 3 Schematic test set-up in the laboratory (left) and at the real electric vehicle (right)

3 Insertion Algorithm

Before definition and parametrization of the search algorithm, first step is to roughly determine the error values of poses estimated by vision system to learn the size of the necessary search area. In Table 1 there are the average values, the standard deviation and the maximum values of the measured displacements for all translational and rotational DOFs. The values were determined during 25 repetitions of visual detection. These displacements have to be compensated for successful insertion. Humans perform similar tasks absolute intuitively and can even do it without any visual information. Humans feel the contact forces if the plug does not fit and adjust it to the socket without much problems. The idea is to use the compliant behavior of the LWR iiwa to imitate human behavior. For making robot's behavior compliant we use impedance control. Here, the impedance Z models the relationship between forces and positions. It is defined by means of the inertia matrix M, the damping matrix D and the stiffness matrix K. The controller input is the desired force $\vec{F}_d$ and the actual measured force $\vec{F}$. Concerning the inputs and the desired impedance, the corrective position $\vec{x}_c$ results. This position and the desired position $\vec{x}_d$ add up to the commanded target position $\vec{x}_t$ (Fig. 4). The robot's behavior is based on a 6-dimensional spring-damper system. The controller strains the spring until $\vec{F}_d$ is reached. If $\vec{F}_d$ is exceeded the robot yields to the forces.

Table 1 Displacement Values due to Vision System

DOF	Average of errors	Standard deviation	Maximum Error
x	0.61 mm	1.09 mm	4.10 mm
y	1.16 mm	1.77 mm	3.03 mm
z	2.36 mm	2.16 mm	7.35 mm
Ψ	3.01 °	0.64 °	5.10 °
Θ	2.81 °	0.88 °	4.51 °
ϕ	2.40 °	0.72 °	4.67 °

$$\vec{x}_t = \vec{x}_d + \vec{x}_c$$
$$\vec{x}_c = Z(s)^{-1} \cdot \left(\vec{F}_d - \vec{F}\right) = (Ms^2 + Ds + K)^{-1} \cdot \left(\vec{F}_d - \vec{F}\right) \quad (1)$$

Our algorithm (Algorithm 1) consists of three steps. Initially (line 5)) it is searched for the contact between the plug and the surface of the socket in z-direction. The second step (line 6) is a compensation of displacement between a pose of the plug and a pose of the socket, i.e. in this step we implement the main part of the search algorithm. In the third step (line 8) the required force is generated for complete insertion while small remaining displacements are compensated. Below these three steps will be explained in detail.

Algorithm 1. Insert the plug into the socket

```
    Input: Stiffness and damping values for compliance
           plus frequencies and force amplitudes for the
           search motion & values of break conditions
1     K[],D[];  //stiffness and damping values
2     sz_f;     //distance in z for successful searching
3     sz_in;    //required distance for complete insertion
    Output: was insertion process successful or not
4     success=false;
5     move towards the socket until impact force occurs;
6     compensate uncertainties by executing compliant
      search motion;
7     if sz>=sz_f then
8         generate required force for complete insertion;
9         if sz==sz_in then
10            success=true;
11        endif;
12    endif;
13    return success;
```

3.1 Find Contact with Socket Surface

After the visual system localized a rough pose, the plug should be 30 mm in front of the plug socket (z-direction). As Table 1 illustrates this value will contain errors. Searching for the first contact compensates this error. First impact is an older research problem and many approaches deal with it, e.g. [17], [18]. By means of impedance control, bouncing due to the impact is avoided. Making the robot's behavior very compliant in contact direction ($K_z = 50\,N/m$) leads to smooth contact until the force *Fz* is equal or greater than a defined contact force (break condition, *Fz*=3N). The robot already reacts to quite low forces and thereby avoids bouncing.

3.2 Compensate Pose Displacements

The control system of LWR iiwa allows Cartesian impedance control with additional forces/torques $\vec{F}_{add}$ [16]. In the following 'forces' includes also 'torques'. The additional forces lead to desired deviations from the proper path. This can be used as a search strategy. The additional forces influence $\vec{F}$ (compare eq. (2) and (1)):

$$\vec{x}_c = Z(s)^{-1} \cdot \left[\vec{F}_d - \left(\vec{F} + \vec{F}_{add}\right)\right] \tag{2}$$

It is also possible to add constants or changing forces in every degree of freedom. Thus, many different paths can be created on the tip of the charging plug (TCP). A number of parameters (stiffness K_i, frequency f_i, force amplitude A_i and the relative robot velocity v_{rel}) affect the path. This will be explained in the following. In our work, we use additional forces to generate a compliant blind-search strategy. For active compensation of the errors we add sinusoidal forces in x- and y- directions and a sinusoidal torque around *z*, i.e. ψ (eq. (3)). The errors in the other DOFs are compensated in a passive way [13], i.e. the robot behaves compliantly in these DOFs, but there are no additional forces and thus no active searching motions. That is why we talk about active and passive compensation. The following equations result according to [19].

$$\begin{bmatrix} F_{add_x} \\ F_{add_y} \\ F_{add_\psi} \end{bmatrix} = \begin{bmatrix} A_x \cdot sin\left(\frac{2\pi \cdot f_x}{v_{rel}} \cdot t\right) \\ A_y \cdot sin\left(\frac{2\pi \cdot f_y}{v_{rel}} \cdot t\right) \\ A_\psi \cdot sin\left(\frac{2\pi \cdot f_\psi}{v_{rel}} \cdot t\right) \end{bmatrix} \tag{3}$$

From the above forces, the search paths for the active coordinates arise:

$$\begin{bmatrix} x(t) \\ y(t) \\ \psi(t) \end{bmatrix} = \begin{bmatrix} \frac{1}{2}\left(F_{add_x}/K_x\right) \\ \frac{1}{2}\left(F_{add_y}/K_y\right) \\ \frac{1}{2}\left(F_{add_\psi}/K_\psi\right) \end{bmatrix} = \begin{bmatrix} \frac{1}{2}(A_x/K_x) \cdot sin\left(\frac{2\pi \cdot f_x}{v_{rel}} \cdot t\right) \\ \frac{1}{2}(A_y/K_y) \cdot sin\left(\frac{2\pi \cdot f_y}{v_{rel}} \cdot t\right) \\ \frac{1}{2}(A_\psi/K_\psi) \cdot sin\left(\frac{2\pi \cdot f_\psi}{v_{rel}} \cdot t\right) \end{bmatrix} \tag{4}$$

To get a phase shifted Lissajous formed path in the xy-plane the frequency ratio is defined as:

$$f_y/f_x = 0.4 \tag{5}$$

This ratio effects a periodic wave motion, which covers a complete rectangle (Fig. 6) [20]. For comparison, if we used a spiral motion the search area would only cover a circle inside the rectangle without any corners.

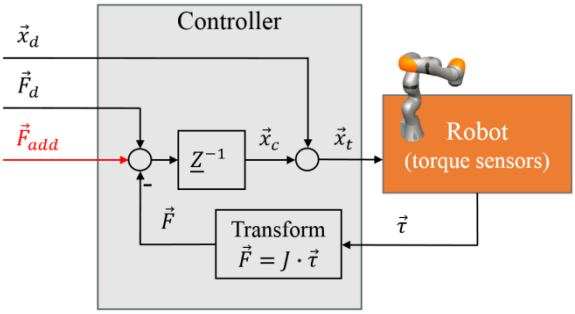

Fig. 4 Block Diagram of Impedance Control with Additional Force $\vec{F}_{add}$ ($\vec{\tau}$: measured joint torques, J: Jacobian)

To obtain a robust search strategy the size of the search area is greater than the maximum displacements listed in Table 1. We use the following values for the impedance parameters carry out the passive and the active compensation. The search path shown in Fig. 5 is generated because of the red marked values.

$$\left(K_x\ K_y\ K_z\right)^T = (300\ \ 300\ \ 1000)\ N/m \qquad \left(K_\psi\ K_\theta\ K_\phi\right)^T = (10\ \ 10\ \ 10)\ Nm/rad$$

$$\left(A_x\ A_y\ A_z\right)^T = (6\ \ 6\ \ 0)\ N \qquad \left(A_\psi\ A_\theta\ A_\phi\right)^T = (3.4\ \ 0\ \ 0)\ Nm$$

$$\left(f_x\ f_y\ f_z\right)^T = (5\ \ 2\ \ 0)\ Hz \qquad \left(f_\psi\ f_\theta\ f_\phi\right)^T = (6\ \ 0\ \ 0)\ \mathrm{Hz}$$

$$\Delta x = \Delta y = \frac{A_{x/y}}{K_{x/y}} = \frac{6}{300}\ m = 20\ mm \tag{6}$$

$$\Delta\psi = \frac{A_\psi}{K_\psi} = \frac{3.4}{10}\ rad \approx 19.5° \tag{7}$$

The stiffness *Ki* and the force amplitude *Ai* of x and y determine the maximum deviation of the search path (eq. (6)). It is similar to ψ (eq. (7)). The frequency of sine wave in *fx* -direction is chosen because of experimental tests. Thereby *fy* results from eq. (5) and *fψ* is chosen higher than *fx* in order to have a phase shift between the Lissajous figure in xy-plane and the sinus wave in ψ.

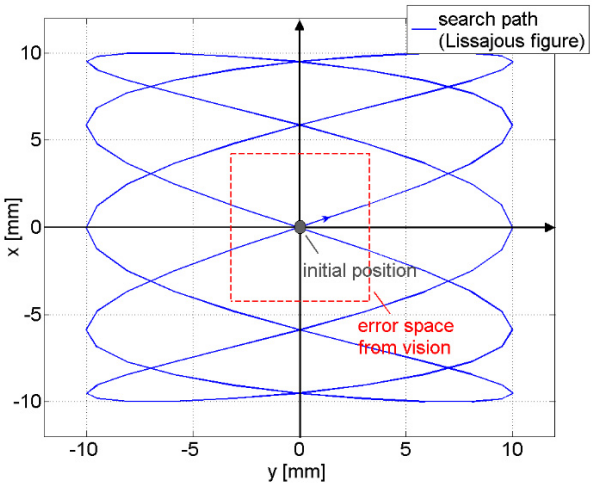

Fig. 5 Blind-Search-Path on the XY-Plane due to additional forces. The initial position is the position which comes from the socket detection by vision system. The red rectangle represents the maximum error area measured by the vision system, i.e. the socket should be inside the area

Starting from the initial pose $(x_0; y_0; z_0; \psi_0; \theta_0; \phi_0)$ with given parameter values, the search area covers the following region:

- $-10\,mm \leq x_0 < 10\,mm$ because of $\Delta x = 20\,mm$
- $-10\,mm \leq y_0 < 10\,mm$ because of $\Delta y = 20\,mm$
- $-9.75\,° \leq \psi_0 < 9.75\,°$ because of $\Delta\psi \approx 19.5°$

3.3 Generate Required Force to Complete the Insertion

The third step starts if the socket is found in the previous step. The criterion is the distance covered in the *z*-direction. If it is too small, it means that the plug remains on the surface of the socket. If the value is greater than 10 mm, we assume the socket has been found. Another indicator is the development of forces. This is explained in more detail in the next section. If the criterion is fulfilled a new impedance control will be parameterized. All DOFs stay compliant except in *z*-direction. The stiffness for z becomes $K_z = 4000\,N/m$. This configuration allows the generation of the required force in insertion direction and simultaneously

further passive compensation of pose errors in the other DOFs. The insertion is finished when the distance *sz* has reached the depth value of the socket *sz_in*. In Fig. 6 the complete process is shown schematically.

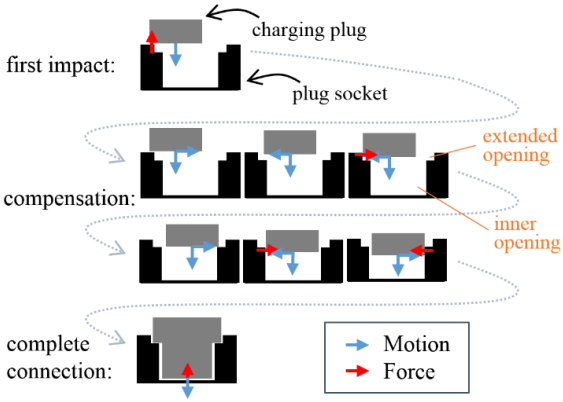

Fig. 6 Schematic Connection Process. The red arrows show the acting forces because of the blue marked motions of the robot and the plug.

The error in the *z*-direction is compensated during the first step of algorithm (sec. 3.1 - first impact). The rotational errors in θ and ϕ are compensated due to compliance without active motions. The search motion and the slow linear motion in *z*-direction will lead to collisions with the inner side of the socket. These contacts in combination with the compliant behavior of the robot effect the gradual adaption of the socket´s pose and carry out the alignment with the socket pose. This phase is successful when the distance covered in *z*-direction *sz* is greater than the specified limit value *sz_f* (sec. 3.2 - compensation). Full connection is created in the third step.

4 Experiments and Results

A series of experiments has been carried out to evaluate the performance of the proposed algorithm. During the first test phase at laboratory set-up (Fig. 3) the positioning errors of the plug are varied up to the boundary of the search path area (Fig. 5). We consciously exceeded the expected errors from the vision system (Table 1) for testing the robustness of our approach. In a second phase, we evaluate our search algorithm together with the vision system on a real electric vehicle (Fig. 3). Additionally we tested the presented approach for another kind of plug to show the transferability.

Much more than 100 different start positions were tested in test phase one. If the initial errors are inside the actively searched area (x, y, ψ) and inside the maximum errors of θ and ϕ the insertion was always successful. The active compensation reliably corrects 8 mm in x and y respectively 8° in ψ. The passive

compensation corrects up to 5° in θ and ϕ. For making it more robust it is possible to integrate an active search as it is realized for ψ. But this is not necessary because the errors will not become such high in the real application. Hence, the laboratory test phase was successful and has demonstrated robustness of the algorithm. After these tests it was evaluated together with the vision system at a real car, i.e. the initial position was determined by image processing. As it was expected, there were no failures because the positioning by the vision system is much more accurate than our test positions during laboratory evaluation. We tested it again more than 100 times and if the socket was detected by vision the following insertion was always successful. Thus, we proved the functionality of the suggested insertion algorithm. In the following we will explain the process of one trial, representative for all of them.

In the time response of the position (Fig. 7, left), the blind-search phase is visible because before the robot is moving forward in z-direction it only moves within the xy-plane. The size of the scanned area (blue curve in the xy-plane in Fig.7, left) is much smaller than it is shown in Fig. 5, because at the beginning of step 2 (compensation of the pose errors) the plug is already inside the extended opening of the socket (Fig. 6). The right plot of Fig. 7 shows a slow increase in *Fz* after three seconds, while *Fx* and *Fy* still alternate but now with higher amplitudes. The higher maximum values for *Fx* and *Fy* indicates that the search motion is even more limited. Looking for this in the plot of position (Fig. 7, left), we see the limitation really increases when the robot moves forward in z-direction. At this moment the plug enters the inner opening of the socket. The increase of *Fz* results from the slow linear motion in z-direction and the straining of the virtual spring-damper-system.

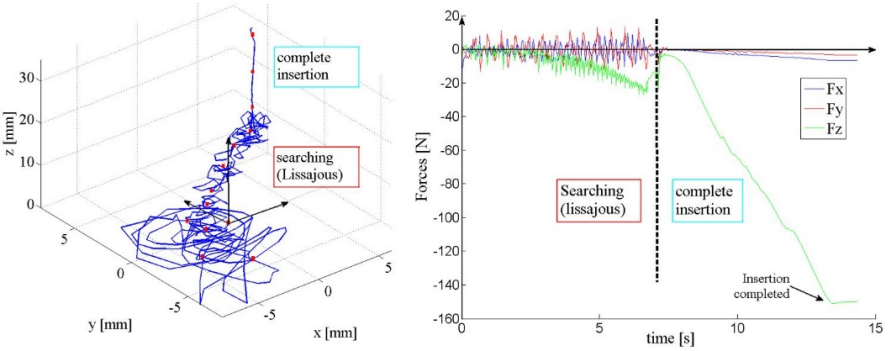

Fig. 7 Left plot: 3D position of the plug during insertion process. Right plot: Forces in translational DOFs at the plug during the insertion process

When *Fz* or the distance in z-direction reach their limits the search phase ends. In the presented test, the distance *sz* triggered the stop condition, i.e. the searching was successful. After that the final insertion phase is started. As described in previous sections the algorithm sets the robot very stiff in z-direction and thus it is

able to build up the required force. This happens gradually to prevent the robot and the environment from damage. Now *Fz* becomes slowly greater while the other forces stay nearly at zero level (Fig. 7, right)). Transition from step 2 to step 3 is also visible in the position plot of Fig. 7. This is when it becomes nearly the simple straight line parallel to the z-axis. Presently, the algorithm stops in step 3 when the specified distance sz_i is reached. In the future, there will be a digital signal generated when the insertion is completed.

During the whole insertion process the joint torques of the robot are checked for excessive values. This is very important for safety and indispensable for detection of problems and prevention from damage. Additionally, in the final version of the charging station there will be a camera for controlling the global workspace. It will be able to stop the robot if any danger for human or machine is detected, when e.g. a human moves into robot's workspace.

To show the adaptability to other kinds of plugs and other application we test the algorithm for insertion of a heavy current plug (Fig. 8). As expected it works when we adjust the amplitudes of the search paths and the value of the generated force during the insertion phase. The adjustment mainly affects the frequency of the searching path around the z-axis and the Lissajous oscillation in xy-plane. It should be decreased because the notch is comparatively hard to find due to the small clearance (< 0.5mm).

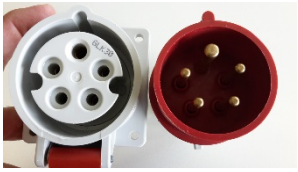

Fig. 8 Socket (left) and plug (right) for a heavy current connection. It is visible that a small notch guarantees the suitable connection, i.e. the absolutely correct pose has to be found by the algorithm. There is only a very small clearance value (< 0.5 mm) between plug and socket.

5 Conclusion

In this paper we presented a method for a peg-in-hole task where the pegs are charging plugs for electric vehicles. The plug has 7 pins, which is very challenging. We used a robot with programmable compliant behavior. Based on this possibility we implemented a compliant blind-search strategy. The algorithm starts after the robot receives a coarse position of the socket from the vision system. The functionality was verified by numerous experiments. They prove, our approach is able to compensate the expected position errors between the plug and the socket and the robustness of the algorithm is much higher than actually requested by means of Table 1. Thus, the success rate for realistic initial error values was up to 100%. If the error values are different in other applications, the search area can be adjusted by changing the parameters of the additional forces.

We suggest verifying this approach in the future for other settings because it can be easily transferred to other tasks when the estimation of coarse pose is available. The developed algorithm can be easily adapted to solve similar problem which frequently occur in assembly or service robotics. One of them can be the establishing of a heavy current connection which was successfully tested during the presented research project.

References

1. Fuelmatics Systems AB, July 5, 2015. http://fuelmatics.com/
2. RotecEngineering, July 5, 2015. http://rotec-engineering.nl/en/automation/refueling-robot/
3. GINKO, June 28, 2015. https://www.tu-chemnitz.de/etit/sse/Forschung/Projekte/ginko.html
4. Whitney, D.E.: Quasi-static-assembly of compliantly supported rigid parts. In: Journal of Dynamic Systems, Measurement and Control Division, pp. 65–77 (1981)
5. Sharma, K., Shirwalkar, V., Pal, P.K.: Intelligent and environment-independent Peg-In-Hole search strategies. In: 2013 International Conference on Control, Automation, Robotics and Embedded Systems (CARE), pp. 1–6, December 16–18, 2013
6. Chhatpar, S.R., Branicky, M.S.: Localization for robotic assemblies with position uncertainty. In: Proceedings of the Intelligent Robots and Systems, (IROS 2003), vol. 3, pp. 2534–2540 (2003)
7. Newman, W.S., Zhao, Y., Pao, Y.-H.: Interpretation of force and moment signals for compliant peg-in-hole assembly. In: Proceedings of the 2001 IEEE International Conference on Robotics and Automation, ICRA, vol. 1, pp. 571–576 (2001)
8. Thomas, U., Molkenstruck, S., Iser, R., Wahl, F.M.: Multi sensor fusion in robot assembly using particle filters. In: 2007 IEEE International Conference on Robotics and Automation, pp. 3837–3843 (2007)
9. Yamamoto, Y., Hashimoto, T., Okubo, T., Itoh, T.: Task analysis of ultra-precision assembly processes for automation of human skills. In: Proceedings of the 2001 IEEE/RSJ International Conference on Intelligent Robots and Systems, vol. 4, pp. 2093–2098 (2001)
10. Savarimuthu, T.R., Liljekrans, D., Ellekilde, L.-P., Ude, A., Nemec, B., Kruger, N.: Analysis of human peg-in-hole executions in a robotic embodiment using uncertain grasps. In: 2013 9th Workshop on Robot Motion and Control (RoMoCo), pp. 233–239 (2013)
11. Goto, T., Takeyasu, K., Inoyama, T.: Control Algorithm for Precision Insert Operation Robots. Transactions on Systems, Man and Cybernetics **10**(1), 19–25 (1980)
12. Stemmer, A., Albu-Schaffer, A., Hirzinger, G.: An analytical method for the planning of robust assembly tasks of complex shaped planar parts. In: 2007 IEEE International Conference on Robotics and Automation, pp. 317–323 (2007)
13. Park, H., Bae, J.-H., Park, J.-H., Baeg, M.-H., Park, J.: Intuitive peg-in-hole assembly strategy with a compliant manipulator. In: 2013 44th International Symposium on Robotics (ISR), pp. 1–5 (2013)
14. Liu, S., Liu, C., Liu, Z., Xie, Y., Xu, J., Chen, K.: Laser tracker-based control for peg-in-hole assembly robot. In: 2014 IEEE Annual International Conference on Cyber Technology in Automation, Control, and Intelligent Systems (CYBER), pp. 569–573 (2014)

15. Song, H.-C., Kim, Y.-L. Song, J.-B.: Automated guidance of peg-in-hole assembly tasks for complex-shaped parts. In: Intelligent Robots and Systems (IROS 2014), pp. 4517–4522 (2014)
16. Albu-Schaffer, A., Ott, C., Frese, U., Hirzinger, G.: Cartesian impedance control of redundant robots: recent results with the DLR-light-weight-arms. In: Proceedings of the IEEE International Conference on Robotics and Automation, ICRA 2003, vol. 3, pp. 3704–3709 (2003)
17. Wu, Y., Tarn, T., Xi, N., Isidori, A.: On robust impact control via positive acceleration feedback for robot manipulators. In: Proceedings of the 1996 IEEE International Conference on Robotics and Automation, vol. 2, pp. 1891–1896 (1996)
18. Bdiwi, M., Winkler, A., Suchy, J., Zschocke, G.: Traded and shared vision-force robot control for improved impact control. In: 2011 8th International Multi-Conference on Systems, Signals and Devices (SSD), pp. 1–6 (2011)
19. KUKA Sunrise.Workbench1.1, Manual, KUKA Laboratories GmbH 2014, pp. 304–305 (2014)
20. Wikibooks, September 17, 2015. http://en.wikibooks.org/wiki/Trigonometry/For_Enthusiasts/Lissajous_Figures